Appl. Phys. B 69, 445–453 (1999) / Digital Object Identifier (DOI) 10.1007/s003409900187

Applied Physics B
Lasers
and Optics

The effect of preparation technique on the optical parameters of biological tissue

A. Roggan[1], **D. Schädel**[1], **U. Netz**[1], **J.-P. Ritz**[2], **C.-T. Germer**[2], **G. Müller**[1]

[1] Institute for Medical Physics and Laser Medicine, Free University Berlin, Krahmerstr. 6–10, 12207 Berlin, Germany
(Fax: +49-30/8449-2399, E-mail: a.roggan@lmtb.de)
[2] Department of General-, Vascular- and Thoracic Surgery, Free University Berlin, Hindenburgdamm 30, 12200 Berlin, Germany

Received: 29 June 1999/Revised version: 1 October 1999/Published online: 3 November 1999

Abstract. The absorption coefficient μ_a, the scattering coefficient μ_s, and the scattering anisotropy factor g of porcine liver were studied in vitro using the integrating sphere technique and inverse Monte Carlo simulation in the wavelength range 450 to 700 nm. A reference preparation technique was developed using a dermatome providing specimens of 200 to 800 μm thickness without pre-freezing the tissue. The optical parameters as measured applying the reference preparation were compared to those measured after cryo-homogenisation. We found significant deviations of the scattering coefficient and the anisotropy factor which were compensated when the reduced scattering coefficient μ_s' was calculated. We also compared the effects of freezing reference specimens at −20 °C and at 77 K without homogenisation. For both freezing protocols noticeable deviations were found in all three optical parameters as well as in μ_s'. The impact of tissue storage at 4 °C was measured in the range 4 to 48 h post mortem and showed a clear reduction of μ_a and a significant increase of μ_s even after 24 h of storage. Short-time storage of the specimens in saline solution reduced all three optical parameters significantly. In conclusion, the tissue preparation must be controlled in order to provide in vitro optical parameters that sufficiently mimic the in vivo situation.

PACS: 42.10; 42.20; 78; 87

First applications of laser radiation in medicine were governed by the clinical and experimental experience of physicians. However, within the last twenty years a better understanding of light distribution in turbid media has been attained, providing a precise prediction of laser-tissue interactions and the optimisation of clinical laser applications. The underlying mechanism of light transport in absorbing and scattering media was adapted from nuclear physics where Chandrasekar calculated the fluence of neutrons through different materials [1]. Hence in most medical laser applications light is regarded as a particle and not as a wave. The integro-differential equation describing the stationary photon transport is given by [2–4]

$$\frac{\mathrm{d}L(\boldsymbol{r},\boldsymbol{s})}{\mathrm{d}s} = -(\mu_a+\mu_s)L(\boldsymbol{r},\boldsymbol{s}) + \frac{\mu_s}{4\pi}\int_{4\pi} p(\boldsymbol{s},\boldsymbol{s}')L(\boldsymbol{r},\boldsymbol{s})\mathrm{d}\Omega' + S(\boldsymbol{r},\boldsymbol{s})\,, \tag{1}$$

where $L(\boldsymbol{r},\boldsymbol{s})$ in $\mathrm{Wcm^{-2}sr^{-1}}$ denotes the radiance at position $\boldsymbol{r}$ into direction $\boldsymbol{s}$ and $S(\boldsymbol{r},\boldsymbol{s})$ in $\mathrm{W\,cm^{-3}}$ is the source term describing the injection of photons. Here, μ_a is the absorption probability per pathlength, μ_s is the scattering probability per pathlength, and $p(\boldsymbol{s},\boldsymbol{s}')$ denotes the scattering phase function. Absorption takes place at chromophores, proteins, and water. Scattering is a result of inhomogeneities of the refractive index at membranes and lipids. The scattering phase function characterises the angular distribution of scattering events and is normalised according to

$$\int_{4\pi} p(\boldsymbol{s},\boldsymbol{s}')\mathrm{d}\Omega' = 1\,. \tag{2}$$

An important question is the choice of a scattering phase function that fits best to the investigated medium. In biomedical optics the Henyey–Greenstein phase function [5] was most often used because it corresponds well to goniophotometric measurements of tissue such as skin or parenchymatous organs [6–12]. The function was first applied in astrophysics for the scattering of interstellar dust and is given by

$$p(\boldsymbol{s},\boldsymbol{s}') = \frac{1-g^2}{4\pi(1+g^2-2g\cos\Theta)^{\frac{3}{2}}}\,, \tag{3}$$

where g is the free parameter which equals the mean cosine of the scattering angle Θ, known as the anisotropy factor that ranges from -1 (total back scattering) over 0 (isotropic scattering) to +1 (total forward scattering).

$$g = \langle\cos\Theta\rangle = \int_0^{2\pi}\mathrm{d}\Phi\int_0^{\pi} p(\boldsymbol{s},\boldsymbol{s}')\cos\Theta\sin\Theta\mathrm{d}\Theta \tag{4}$$

The use of some analytical models for the calculation of the fluence does not require the separate consideration of μ_s and g, especially if absorption is small compared to scattering and the fluence is regarded far from boundaries and sources. In this diffusion regime, anisotropic scattering can be simplified to the isotropic case by applying the similarity relation [13]:

$$\mu_s' = \mu_s(1-g)\,, \tag{5}$$

where μ_s' denotes the reduced scattering coefficient.

In summary, the optical parameters of biological tissue are given by the absorption coefficient μ_a, the scattering coefficient μ_s, and the anisotropy factor g, using a selected scattering phase function. There exist a number of possible strategies for their evaluation. In principle, a classification into *direct* and *indirect* methods is possible [14–16]. Direct techniques are based on the assumption of Beer's law: light is attenuated exponentially at its propagation in tissue and there is no dependence on mathematical models of transport theory. Measurements of unscattered (collimated) transmission belong to this group but can only provide the total attenuation coefficient

$$\mu_t = \mu_a + \mu_s\,. \tag{6}$$

In contrast, indirect methods also measure the diffuse radiation emerging from the tissue sample into the backward and/or forward hemispheres. The method that is most frequently applied in vitro to determine the complete set of optical parameters of turbid media (such as biological tissue) is the integrating-sphere technique [17–25]. With collimated illumination, measurement of the diffuse reflectance (R_d), the total transmittance (T_t), the collimated (mostly unscattered) transmittance (T_c), and the thickness of a specimen permits the complete determination of its optical parameters (Fig. 1). Nevertheless, it is an experimental challenge to obtain high-precision results with this technique because a number of difficulties have to be considered:

A. Typical attenuation coefficients of soft tissue cover the range $10\,\mathrm{mm}^{-1}$ to $50\,\mathrm{mm}^{-1}$ at visible wavelengths [15]. Consequently, the specimen thickness should be in the range $500\,\mu\mathrm{m}$ down to $100\,\mu\mathrm{m}$ in order to sample at least a few ballistic photons at the T_c detector. However, thin samples suffer from a minor diffuse reflectance that may considerably be less than 1%, especially if absorption is high compared to scattering. This effect combines with the use of integrating spheres which again reduce the amount of light measured at the detectors. Although the intensity of the radiation field inside the integrating sphere is increased due to multiple reflections (a typical value is a factor of ~ 30 for a 150-mm diameter with a reflection factor of 98% and a 1% surface fraction of non-reflecting holes), the detector surface of approximately 5 mm diameter makes up only 1/3000 of the sphere surface. As a consequence the diffuse radiation emerging from the specimens is additionally attenuated by two orders of magnitude so that a dynamic detection range of at least 6 orders of magnitude is required. It should be noted that highly reflecting baffles or detectors with a small field of view are used in order to avoid the direct illumination of the detectors.

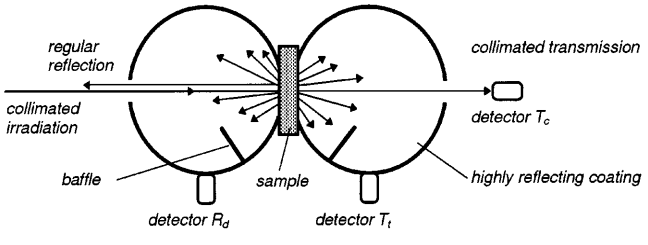

Fig. 1. Schematic diagram of an integrating-sphere experiment

B. Previous investigations were carried out with a double-sphere system, measuring reflectance and transmission simultaneously [22–25]. This procedure is fast but bears a significant interaction of the two radiation fields, yielding a virtual increase in the measured quantities. Pickering et al. developed an algorithm that allows for a compensation of this effect, but one requires precise knowledge about the sphere-wall reflectance [20, 21]. On the other hand, the mean wall reflectance is difficult to measure and unstable due to dust and partial contamination. Hence, the compensation is only a poor approximation for specimens with a small optical thickness. A minor problem with double-sphere systems is the necessity to correct the measurements according to the integrating-sphere equations because the reflection standard must be replaced by the sample when changing from calibration to measurement. The corrections also require knowledge about the sphere-wall reflectance, only being available with a relatively large error. To overcome these difficulties a single-sphere arrangement can be applied as described in Sect. 1.1.

C. A problem arises from the T_c measurement because a total separation between ballistic and scattered photons is not possible. The diffuse transmission of a sample always produces an offset at the T_c detector that only depends on the detected solid angle. In theory, the solid angle can be reduced by increasing the distance between detector and specimen or by the use of a smaller aperture in front of the T_c detector. In practice this is limited by the beam quality which is often established by a monochromator in order to easily scan over large wavelength ranges. With a typical beam divergence of 0.2 rad about 0.4% of the diffuse transmission hits the T_c detector. Taking into consideration that the diffuse transmission is the most dominant value of all three measured quantities, it is evident that more than 50% of the T_c readings can be affected by scattered photons. The only way to handle this problem is the use of evaluation models that allow compensation of the described phenomenon.

D. A further problem appears with scattered photons travelling to the side boundaries of the specimen. Because the radial dimension of the specimen is limited by the sphere port diameter or the cuvette geometry (or the clinically available tissue volume), a significant amount of photons may travel to the sides being neither detected in transmission nor in reflectance. Consequently, the ratio between spot size and sample diameter should be as small as possible in order to minimise this effect. Nevertheless, typical configurations show side losses of up to 15% in the near infrared where scattering clearly domi-

nates over absorption. As a consequence the side losses can only be compensated for by sophisticated evaluation models.

E. An important point of consideration is the handling of the regular reflection at the cuvette glass or the specimen itself. By tilting the sample about 8° relative to the optical axis, all regular reflexes can either be measured as offset on the diffuse reflectance or leave the integrating sphere through an additional hole. However, since the regular reflection makes up about 3% in the visible wavelength range, a precise control appears to be necessary.

Extraction of the optical parameters from the described measurements is a complex task as there is no exact analytical solution for the transport equation (1) available. A frequently utilised approach is the Kubelka–Munk theory [26] or the more sophisticated diffusion approximation of the transport equation [2, 13, 27, 28]. But these one-dimensional models suffer from boundary conditions (infinite sample extension, absorption must be small compared to scattering) which can not be realised in practical measurements [29]. Besides, all of the above-mentioned systematic error sources (diffuse photons at T_c, side-travelling photons in the specimen, regular reflection at the cuvette) can not be considered in these analytical approaches. Consequently, numerical models are preferred to calculate optical parameters from integrating-sphere measurements. These are the adding-doubling method [3, 4, 9] and the Monte Carlo simulation [30, 31], whereby the former, as a one-dimensional model, also assumes infinite lateral sample extension and neglects most of the systematic errors. In summary, the Monte Carlo simulation is the method of choice, providing the consideration of every aspect of the experimental set-up. The method will be described in detail in Sect. 1.3.

Concluding the previous paragraphs, reliable measurements of the optical parameters of turbid materials are possible at the present time under in vitro conditions. However, it is evident that the optical parameters measured in vitro should mimic the in vivo situation as accurately as possible because these data are used clinically for treatment planning. This requires the use of a sophisticated preparation technique in order to provide constant sample thickness without significant changes of the tissue structure. As a consequence, the tissue preparation must preserve the optical parameters but is often suspected to have an effect on their evaluation. To our knowledge no investigations have been published which apply a high-precision experimental set-up in order to systematically evaluate the effects of tissue preparation and preservation. Therefore, the aim of this study was to compare the impact of different preparation techniques on the determination of absorption, scattering, and anisotropy of soft-tissue specimens.

1 Experimental set-up and methods

1.1 Measurement of reflectance and transmittance

The optical parameters were determined by the integrating-sphere technique, measuring the diffuse reflectance R_d, the total transmittance T_t, and the collimated transmission T_c of various tissue samples (Fig. 1). We applied an experimental set-up with a single-sphere (150-mm diameter, Spectraflect®coating, Labsphere Inc., USA), measuring R_d and T_t subsequently without interactions. For calibration purposes a reflection standard (Labsphere Inc., USA) was mounted into one of the sphere ports and the sample was positioned at another port. The sphere was then rotated by 90° to change illumination between standard and sample. By this procedure no compensation for a varying sphere efficiency was needed. If necessary, the sphere was displaced along the optical axis in order to position the sample in the focal plane of the illuminating light. The procedure for the measurement of all three quantities is shown in Fig. 2. As a special feature we also used integrating spheres with a 30-mm aperture (100-mm diameter, $BaSO_4$ coating) for both T_c and reference intensity measurement. For this reason no focusing lenses were necessary independent of the divergent light beam.

Figure 3 shows the experimental set-up. A mercury high-pressure short-arc lamp served as light source (100 W, 2×10^6 cd/cm^2, Osram, Germany). The lamp was connected to a monochromator ($f = 200$ mm, AMKO, Germany) providing a resolution of 8 nm (FWHM) and measurements in the wavelength range 450–700 nm. The circular monochromator exit (diameter 1 mm) was focused into the sample plane by a spherical mirror, providing a spot size of diameter 4 mm. The distance between sample and T_c sphere was 430 mm, the beam diameter at the aperture of the T_c sphere was 25 mm. The beam was modulated with 220 Hz using a mirrored chopper blade whereby the reflected fraction was used for intensity normalisation. Silicon photodiodes with integrated pre-amplifiers served as detectors (09-SiU04-C, AMKO, Germany), each connected to a separate lock-in amplifier (ITHACO 3981, US). Control of the experiment and guidance through the measurement procedure were entirely computer-controlled.

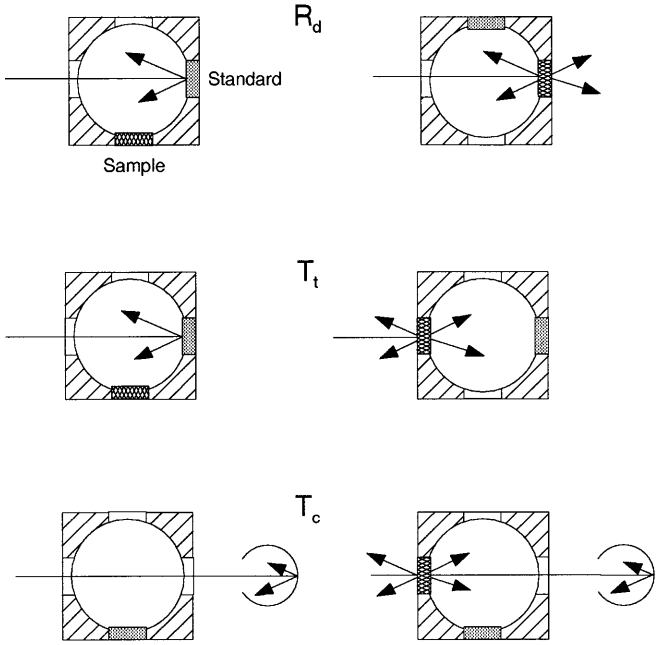

Fig. 2. Scheme of the measuring procedure, *left column*: calibration configuration, *right column*: configuration for tissue measurements

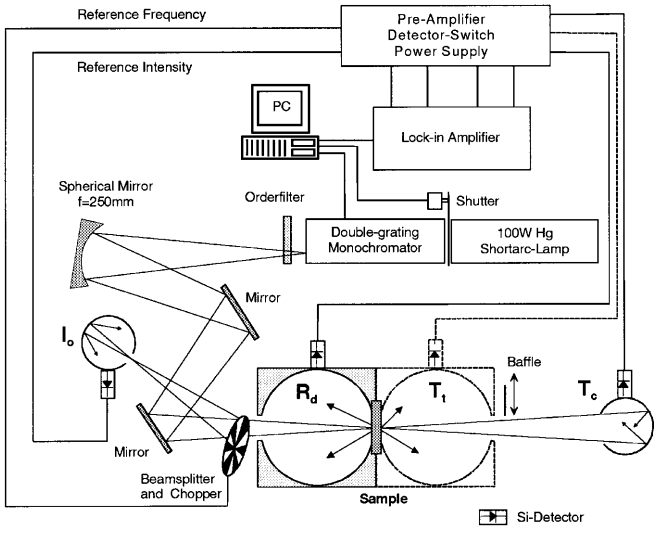

Fig. 3. Experimental set-up

1.2 Tissue preparation

We selected porcine liver as soft-tissue model for the comparison of various preparation techniques and storage procedures. This choice was motivated by the fact that liver tissue is a common model used for the evaluation of various application protocols for laser-induced thermotherapy and for comparison with theoretical models of light and heat distribution [32]. The livers were procured from the slaughterhouse and prepared within 4 h post mortem.

In practice, the reproducible preparation of tissue sections at the required thickness (100–500 μm) is a difficult task. The standard procedure in histology is the use of microtomes that allow sections to be cut from frozen specimens, but their maximum thickness is limited to about 40 μm. Therefore this technique was not applicable for optical parameter evaluation.

An alternative technique that has been applied by some authors especially for soft tissue is cryo-homogenisation [18, 22–25, 33]. Specimens of the fresh liver with a dimension of approximately 5 mm were shock-frozen in liquid nitrogen at 77 K. Then they were carefully homogenised in a precooled mortar. This resulted in tissue clusters with diameters between 20 and 200 μm, being large compared with typical cell dimensions of a few microns. This allows the assumption that the original optical properties of the tissue matrix were mainly preserved. The specimens were prepared into cylindrical quartz cuvettes with a calibrated spacing of 200 ± 5 μm (Hellma, Germany) to provide measurements in the integrating-sphere system. The diameter of the cuvette sample chamber was 15 mm, hence it was large compared to the spot diameter of the light source, keeping the number of side-travelling photons small. The cuvette was finally fixed within a cylindrical holder which directly fitted into the integrating-sphere aperture. The thickness of each sample was determined before each measurement using a calibrated micrometer screw.

Nevertheless, the previously described technique is suspected to alter the optical properties by the damage of membranes due to fast-building ice crystals and mechanical forces. As a result, we have developed a new cutting technique that could serve as a standard for the preservation of in vitro optical parameters of soft tissue. The specimens were directly cut from the fresh liver using a dermatome (Zimmer, USA). This instrument is normally used in plastic surgery to remove superficial layers of healthy skin for transplantation (Fig. 4). A motor-driven knife with a length of 100 mm oscillates horizontally with about 50 Hz. The dermatome was manually moved over the fresh liver, providing layers with a constant thickness that have been pre-set to 200 μm by adjusting the distance between the knife and a spacer. A pre-requisite of this method was the optimal fixation of the whole liver. For this purpose a vacuum table was built that consisted of an acrylic glass plate with boreholes of 1 mm diameter, equally distributed with a mutual distance of 5 mm. The plate covered a chamber that could be evacuated by a connected pump (Fig. 5). The liver was put onto the plate, covering the boreholes. By establishing a vacuum of a few millibars the liver was fixed to the table and the dermatome could easily be moved over the organ without subsequent movement of the tissue. The liver capsule was always removed by the same technique before a layer was selected for measurements. Finally, a cylindrical specimen with a diameter of 15 mm was stamped out of the layer, so that it could directly be prepared into the 200-μm quartz cuvettes as described above. From this technique we assumed that the optical parameters were maintained as well as possible compared to the in vivo situation.

Fig. 4. Dermatome (Zimmer, USA)

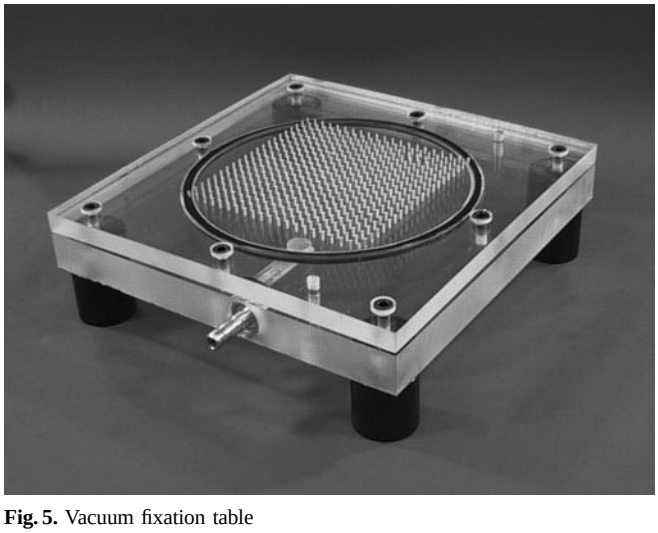

Fig. 5. Vacuum fixation table

Besides the various preparation techniques we also compared the effect of sample storage, often necessary under clinical conditions. Therefore, specimens were cut with the dermatome according to the reference technique and than exposed either to 77 K in liquid nitrogen or to −20 °C in a freezer. Before measurement, the specimens were thawed at room temperature and prepared into the quartz cuvettes as described above. In a second series we compared fresh tissue (4 h post mortem) with tissue that was stored 24 h and 48 h at 4 °C. Here the cryo-homogenisation technique was used because application of the dermatome was not possible. The mechanical structure of the liver after 24 h of storage did not allow for precise cutting due to lysis processes. In addition, it can be found in the literature that specimens are sometimes stored in saline solution before the optical parameters are measured [34–37]. This avoids drying effects during storage and is also recommended if special tissue slicers are used for tissue cutting (for example Krumdiek, USA). Therefore, the cryo-homogenisation was also applied to specimens that were first prepared with the dermatome and then stored in a saline solution for a few minutes at room temperature before further preparation. In all series the tissue specimens were stored in a plastic bag that was evacuated and hermetically closed in order to avoid drying effects.

Each investigation consisted of nine independent measurements: three livers were taken from different animals and three specimens were prepared from each liver in the same way. In total, 63 spectra were measured, allowing the calculation of mean values and standard deviations.

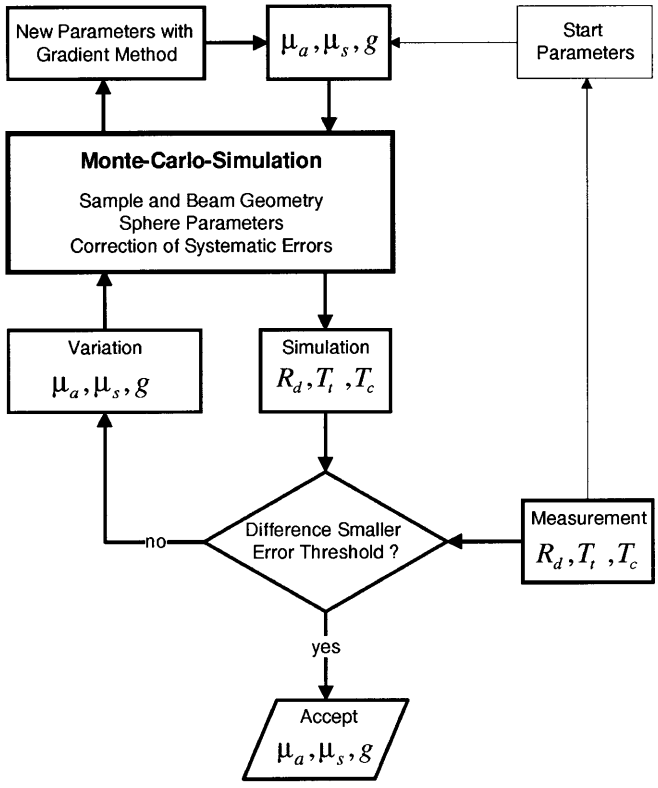

Fig. 6. Scheme of the inverse Monte Carlo simulation developed for the evaluation of optical parameters from reflectance and transmittance measurements

1.3 Numerical evaluation

The optical parameters were determined applying a Monte Carlo simulation, which as a statistical method calculates the trajectories of a great number of photons (3×10^5 in our experiments) and as a result presents the reflectance and transmittance characteristics of a sample for a given set of optical parameters and geometrical configuration. In order to solve the opposite situation, i.e. to determine the unknown optical parameters from the measured macroscopic values, the Monte Carlo simulation was combined with a variation technique [22–25] (Fig. 6). The measured data were simulated taking an estimated set of start parameters μ_a, μ_s, g from Kubelka–Munk theory [26] and applying the Henyey–Greenstein scattering phase function (3). The simulated quantities were compared with the real measurement. In case of a significant deviation, all three parameters were varied slightly and three new forward simulations were performed. After this procedure a gradient matrix was built up, allowing the calculation of new optical parameters which fit better to the measured quantities. This procedure was repeated until the deviation between measured and calculated values was within the error threshold (fixed to 0.1%) so that the associated set of optical parameters could be accepted. As well as a high degree of accuracy the method offered a simple means of compensating systematic errors such as radiation losses, scattered photons detected as collimated transmission, deviations from a Lambertian distribution of the diffuse reflectance, and refractive index mismatches. We utilised a wavelength-dependent refractive index for the quartz cuvettes ranging from 1.466 at 450 nm down to 1.455 at 700 nm [38]. For the liver refractive index we used a fixed value of 1.37 as reported by Bolin et al. for 633 nm [39].

2 Results and discussion

2.1 Preparation with the dermatome

The optical parameters of porcine liver tissue as measured with the reference preparation technique (dermatome) are shown in Fig. 7. The absorption covered one order of magnitude, decreasing from $3.2 \pm 0.2\,\mathrm{mm}^{-1}$ at 450 nm down to $0.25 \pm 0.03\,\mathrm{mm}^{-1}$ at 700 nm. The calculated mean standard deviation of ±8.2% represents the statistical error due to repeated preparation and measurement of specimens of the same organ. At 550 nm a dominant peak with $1.9 \pm 0.2\,\mathrm{mm}^{-1}$ was found which can be related to the strong absorption of deoxygenated haemoglobin [40]. Since there are only a few data for porcine liver published in the literature, comparison is difficult. At 630 nm we found a μ_a of $0.49 \pm 0.04\,\mathrm{mm}^{-1}$, whereas Wilson et al. reported $0.27\,\mathrm{mm}^{-1}$ at the same wavelength using interstitial detectors and diffusion theory [41]. Arnfield et al. reported an absorption coefficient of $0.23\,\mathrm{mm}^{-1}$, also applying interstitial detectors [42]. We found a μ_a of $0.37\,\mathrm{mm}^{-1}$ in previous investigations, using double-integrating sphere equipment [25]. The differences are most certainly the result of the different techniques, regarding preparation, measurement, and evaluation.

The scattering coefficient μ_s slightly decreased with wavelength, showing a maximum of about $19\,\mathrm{mm}^{-1}$ at

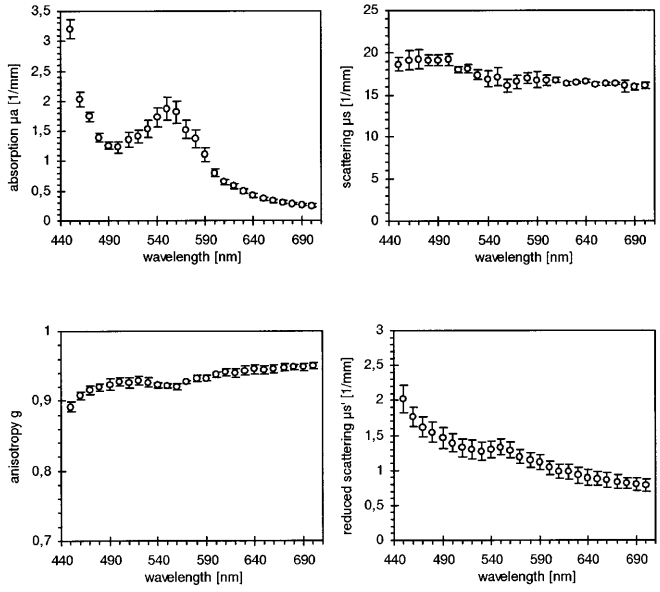

Fig. 7. Optical parameters of fresh porcine liver prepared with the dermatome technique

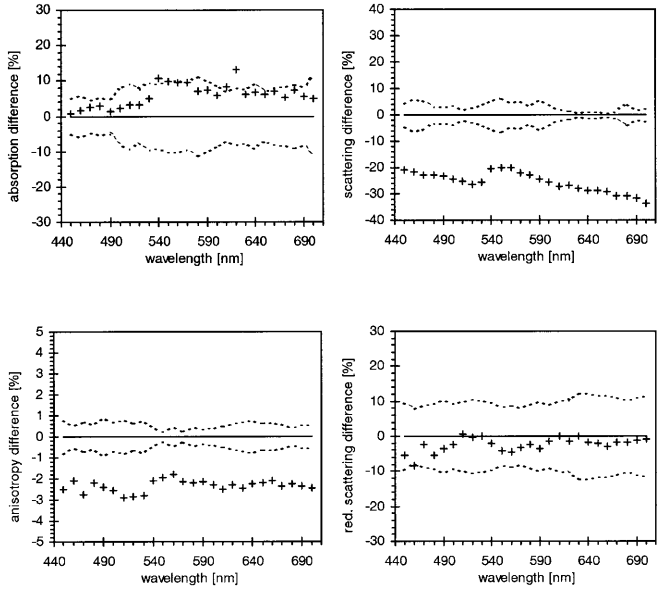

Fig. 8. Relative differences between the optical parameters of fresh porcine liver compared to the reference preparation (dermatome), *crosses*: cryo-homogenisation, *dotted lines*: ± SD for the reference measurements

450 nm and a minimum of 16 mm^{-1} at 700 nm. The mean standard deviation for μ_s was ±3.3%. The decrease of μ_s with increasing wavelength was typical for biological tissue and is related to the theory of Mie scattering. The anisotropy factor g continuously increased from 0.90 at 450 nm up to 0.95 at 700 nm with a mean standard deviation of ±0.6%. This behaviour can also be predicted by Mie theory and is found for many tissue types.

The reduced scattering coefficient μ_s' was calculated according to (5) from the measured data of μ_s and g. The reduced scattering decreased from 2 mm^{-1} at 450 nm down to about 0.8 mm^{-1} at 700 nm with a mean standard deviation of ±9.9%. At 630 nm μ_s' was 0.93 ± 0.1 mm^{-1}, whereas Wilson et al. found 1.7 mm^{-1} [41] and Arnfield reported 1.0 mm^{-1} [42]. Our own data were 0.64 mm^{-1} in previous investigations [25].

It can be seen by comparison with previously published data that the in vitro evaluation of optical parameters is difficult and the obtained results depend on many factors. Moreover, inter-individual variation of the optical parameters are expected [43], complicating the reproducible evaluation. Nevertheless, the measurement of native specimens which were cut with an oscillating knife are expected to produce most precise in vitro results.

2.2 Preparation with cryo-homogenisation

Figure 8 shows the relative deviation of the optical parameters when cryo-homogenisation was applied instead of the dermatome. On average, the absorption level was +5.9% higher after cryo-homogenisation in relation to the reference preparation. However, the differences in μ_a between both preparation techniques lay within the standard deviation of the reference method, consequently they were not regarded as significant. This constant absorption level seems to be evident because no absorbers were removed from the tissue fraction by the cryo-homogenisation itself.

On the other hand, the scattering coefficient μ_s was lowered significantly by −26% on average. The difference in μ_s showed a moderate increase with increasing wavelengths. At the same time, the anisotropy factor g after cryo-homogenisation slightly decreased by −2.3% on average. Here, no wavelength dependence was found. This dramatic change in the scattering properties was expected to be a result of partial damage to membranes and organelles. An additional possibility is the fusion of lipid droplets contained within the cell matrix.

Finally, the calculated reduced scattering μ_s' decreased by a mean value of −3.4%. This decline was not significant compared to the standard deviation of the reference measurement. Hence the changes in μ_s and g compensated each other and no effect due to cryo-homogenisation is expected from our data if the reduced set of optical properties is used (for example in diffusion theory). By comparison, Peters et al. evaluated the effect of homogenisation using human breast tissue by measuring the diffuse reflectance and transmittance [18]. They found a maximum deviation of 3% in comparison to the non-homogenised tissue sections, this being consistent with our measurements. The reported difference was comparable to the deviation between different samples of the same tissue.

2.3 Effect of tissue freezing

Figure 9 demonstrates how freezing of the specimens changed the optical parameters. Shock-freezing at 77 K resulted in a slight decrease of μ_a without a distinct wavelength dependence. The mean reduction was −4.5%, which is not significant. Slow freezing at −20 °C showed the same behaviour but with a more prominent shape. Here μ_a decreased significantly by −14.4%. This decrease in the absorption coefficient after freezing was unexpected because the concentration of absorbers did not change. A possible explanation might be damage to the erythrocytes, especially at slow

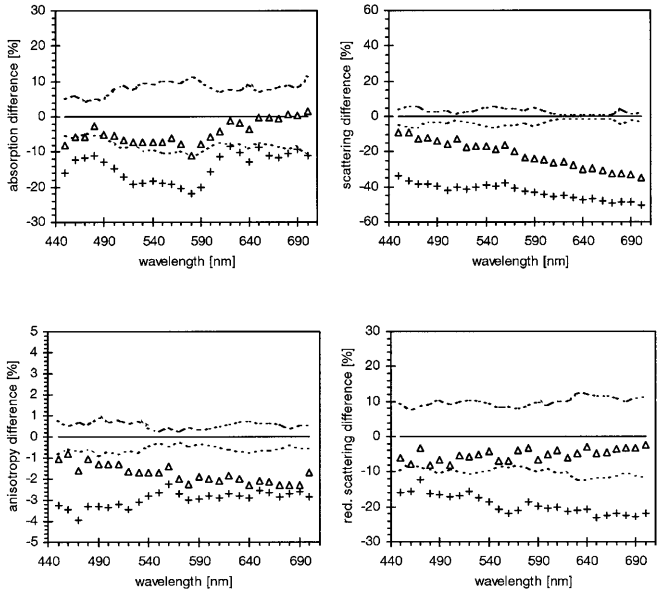

Fig. 9. Relative differences between the optical parameters of fresh porcine liver compared to the reference preparation (dermatome), *crosses*: slow freezing at −20 °C, *triangles*: shock-freezing at 77 K, *dotted lines*: ± SD for the reference measurements

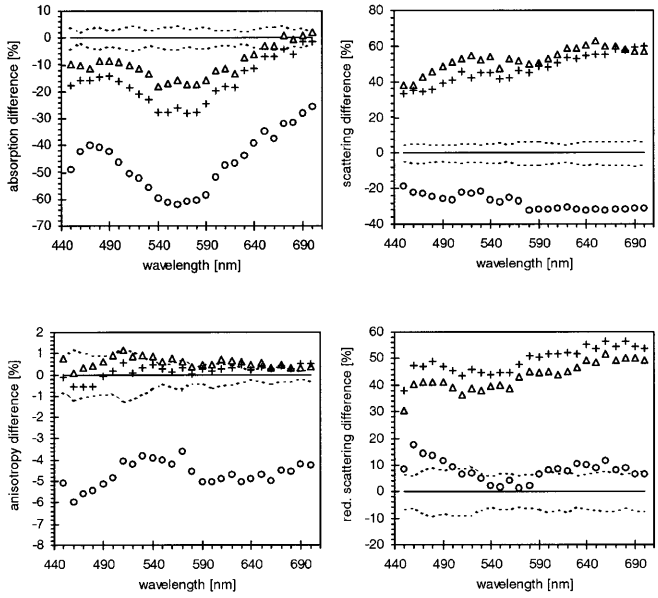

Fig. 10. Relative differences between the optical parameters of porcine liver in comparison to the immediate native measurement (cryo-homogenisation), *triangles*: storage for 24 h at 4 °C, *crosses*: storage for 48 h at 4 °C, *circles*: short preservation in saline solution, *dotted lines*: ± SD for the immediate native measurement

freezing rates, leading to a distribution of free haemoglobin. Cilesiz et al. compared absorption coefficients of aorta before and after freezing and found a decrease in μ_a of −5% to −11% in the range 300 to 800 nm [44]. This was consistent with our measurements.

Shock-freezing led to a significant reduction of the scattering coefficient with a mean decline of −21.7%. The scattering difference showed a clear wavelength dependence with an increasing difference towards longer wavelengths. The anisotropy factor g decreased on average by −1.8%. Finally, the reduced scattering coefficient was lowered by −5.0%, which was not significant compared to the standard deviation. The same behaviour for μ_s, g, and μ_s' was also detected after cryo-homogenisation and has already been discussed. With freezing at −20 °C the scattering coefficient decreased by −42.8% on average and the measurement of the anisotropy factor g led to a mean reduction of −3.0%, showing no significant wavelength dependence. The reduced scattering coefficient was lowered by −19.0% on average with a slight tendency to increasing wavelength. Thus, the effect of freezing on the scattering behaviour is more distinct at −20 °C compared to liquid nitrogen. Peters et al. also compared the effect of freezing at −20 °C on reflectance and transmittance and found a difference of 5% for wavelengths below 600 nm and a difference of 2% above 600 nm [18].

2.4 Effect of tissue storing

Significant changes in the absorption coefficient were found when comparing different storage protocols as shown in Fig. 10. Here the cryo-homogenisation served as reference method because of the difficulty in cutting 'old' liver samples with the dermatome. The mean standard deviation in μ_a was ±3.5% for the cryo-homogenisation of fresh specimens and considerably smaller than that for the dermatome preparation. This was a result of natural inhomogenities of the liver which were conserved when applying the dermatome cutting. On the other hand, tissue homogenisation reduced these inhomogeneities to extensions smaller than our spot size (4 mm diameter) so that the measured standard deviation for repeated measurement was clearly reduced.

Even 24 h of storage at 4 °C resulted in a significant mean decrease in the absorption coefficient of −9.5%. After 48 h of storage the investigated effect was even more pronounced with a mean reduction of −16.4%. From these measurements one can expect that the liver absorption decreases slightly with increasing post mortem 'age'. The underlying mechanism is not understood yet and is probably caused by the transformation of potential absorbers due to processes of lysis. Here haemoglobin plays a major part which can be deduced from the shape of the absorption difference that had a maximum near haemoglobin absorption bands (around 550 nm and towards 420 nm).

24 h of storage led to a significant mean increase in μ_s of +52.7% with an increasing tendency towards longer wavelengths. This had to be compared to the mean standard deviation of ±5.9%, so the increase was highly significant. After 48 h of storage the investigated effects on μ_s did not show a further ageing process since the increase in the scattering coefficient was stable at +47.1% on average. The anisotropy factor g remained nearly unchanged after 24 h as well as after 48 h. Its deviation was within the standard deviation of ±0.6% of the reference measurement. The calculated reduced scattering coefficient μ_s' showed a dominant growth which was +43.3% on average after 24 h and +49.3% on average after 48 h of storage. This resulted from a strong change in the scattering coefficient combined with a constant anisotropy factor. As for the absorption coefficient, the scattering deviation with increasing storage time can only be explained by transformation processes taking place at the tissue matrix.

The most dramatic changes were found when the samples were kept for five minutes in saline solution before

homogenisation and measurement. Here the absorption coefficient decreased drastically by -46.2% on average. The amount of reduction was directly proportional to the absolute value of the absorption coefficient and was expected to be the result of washing out chromophores, mainly haemoglobin. This can be deduced from the fact that the difference was largest in wavelength regions with strong haemoglobin absorption, whereas the changes were clearly smaller in regions with little haemoglobin absorption. The scattering coefficient also decreased significantly by -27.9% on average. Investigation of the anisotropy factor led to a mean decrease of -4.7%. Both effects seemed to compensate each other when the reduced scattering coefficient was calculated from the data of μ_s and g, so that a slight variation of μ_s' was not significant for most of the investigated wavelengths. However, changes in the scattering behaviour could be the result of slightly changing refractive indices in the tissue matrix, being effected by the exchange of ions through the saline solution.

3 Conclusion and summary

The use of a dermatome to make reproducible specimens of biological soft tissue with thicknesses in the range 200 to 800 μm can serve as a reference procedure that does not require freezing or any kind of storage before the measurement. A reliable evaluation of in vitro optical parameters is possible in combination with the integrating-sphere technique and an inverse Monte Carlo simulation which takes systematic error sources into consideration. Even for the same type of tissue the published data of optical parameters cover a wide range. This is due to various preparation techniques, experimental set-ups, and models of evaluation. Hence, the aim of the presented study was to investigate the effect of different preparation techniques and storage procedures under controlled experimental conditions.

No significant differences for μ_a and μ_s' were found when comparing the reference preparation with the frequently applied cryo-homogenisation. Nevertheless, separate investigation of μ_s and g revealed differences in the scattering properties that could be compensated if the reduced scattering was calculated. However, for most clinical applications, knowledge about the reduced set of optical parameters is sufficient for treatment planning so that values measured after cryo-homogenisation can be applied without restrictions.

It can also be concluded from our measurements that the freezing procedure itself changes the optical parameters, especially the scattering properties. The effect is more distinct after slow freezing at -20 °C but can also be seen after shock-freezing in liquid nitrogen. These changes are also compensated for when the reduced scattering coefficient is calculated.

The most substantial variation of all optical parameters was found after storage of the specimens. The changes were already significant 24 h post mortem at 4 °C and only changed slightly within the next 24 h. Consequently it must be concluded that the investigated specimens should be as fresh as possible when the optical parameters are to be measured. Short-time storage of specimens in saline solution must be avoided before measurement because the absorption coefficient changes considerably due to the loss of absorbers, mainly haemoglobin. On the other hand, it is assumed that varying haemoglobin concentrations are the main reason for the wide range of optical parameters measured for the same type of tissue but from different individuals. Consequently, a defined removal of the haemoglobin content might become an interesting procedure in order to increase the reproducibility of optical parameter measurements. To use such parameters for clinical purposes the optical parameters of blood have to be measured separately [45] and must be combined with the blood-free parameters of the interesting tissue by accounting for the actual in vivo blood content. In summary, it is most important to control the preparation conditions in order to determine reliable optical parameters for biological soft tissue.

Acknowledgements. Financial support by the Bundesministerium für Forschung und Technologie (FKZ 13N7064) is gratefully acknowledged.

References

1. S. Chandrasekhar: *Radiative Transfer* (Oxford University Press, London 1950)
2. A. Ishimaru: *Wave Propagation and Scattering in Random Media: Single Scattering and Transport Theory* (Academic Press, New York 1978)
3. H.C. van de Hulst: *Multiple Light Scattering*, Vol. 1 (Academic Press, New York 1980)
4. H.C. van de Hulst: *Multiple Light Scattering*, Vol. 2 (Academic Press, New York 1980)
5. L.G. Henyey, J.L. Greenstein: Astrophysical J. **93**, 70 (1941)
6. S.T. Flock, B.C. Wilson, M.S. Patterson: Med. Phys. **14**(4), 835 (1987)
7. L. Jacques, C.A. Alter, S.A. Prahl: Lasers Life Sci. **1**(4), 309 (1987)
8. M. Arnfield, J. Tulip, M. McPhee: IEEE Trans. Biomed. Eng. **35**, 372 (1988)
9. S. Prahl: *Light Transport in Tissue* (Dissertation, University of Texas at Austin 1988)
10. R. Marchesini, A. Bertoni, S. Andreola, E. Melloni, A.E. Sichirollo: Appl. Opt. **28**(12), 2318 (1989)
11. M.J.C. van Gemert, S.L. Jacques, H.J.C.M. Sterenborg, W.M. Star: IEEE Trans. Biomed. Eng. **36**, 1146 (1989)
12. M. Essenpreis, P. van der Zee, P.S. Jones, P. Gewehr, T.N. Mills: Lasers Surg. Med. **11**(3), 5 (1991)
13. R.A.J. Groenhuis, H.A. Ferwerda, J.J. ten Bosch: Appl. Opt. **22**, 2456 (1983)
14. B.C. Wilson, S.L. Jacques: IEEE J. Quantum Electron. **QE-26**, 2186 (1990)
15. W.F. Cheong, S.A. Prahl, A.J. Welch: IEEE J. Quantum Electron. **QE-26**(12), 2166 (1990)
16. M.S. Patterson, B.C. Wilson, D.R. Wyman: Lasers Med. Sci. **6**, 379 (1991)
17. J. Reichmann: Appl. Opt. **12**(8), 1811 (1973)
18. V.G. Peters, D.R. Wyman, M.S. Patterson, G.L. Frank: Phys. Med. Biol. **35**, 1317 (1990)
19. S.L. Jacques, S. Rastegar, M. Motamedi, S.L. Thomsen, J. Schwartz, J. Torres, I. Mannonen: SPIE Proc. Ser. **1646**, 107 (1992)
20. J.W. Pickering, C.J.M. Moes, H.J.C.M. Sterenborg, S.A. Prahl, M.J.C. van Gemert: J. Opt. Soc. Am. **9**(4), 621 (1992)
21. J.W. Pickering, S.A. Prahl, N. van Wieringen, J.F. Beek, H.J.C.M. Sterenborg, M.J.C. van Gemert: Appl. Opt. **32**(4), 399 (1993)
22. A. Roggan, O. Minet, C. Schroeder, G. Mueller: In *Medical Optical Tomography: Functional Imaging and Monitoring*, ed. by G. Mueller et al. (SPIE Press, Bellingham 1993)
23. A. Roggan, H. Albrecht, K. Doerschel, O. Minet, G. Mueller: SPIE Proc. Ser. **2323**, 21 (1994)
24. A. Roggan, G. Mueller: SPIE Proc. Ser. **2100**, 69 (1994)
25. A. Roggan: *Dosimetrie thermischer Laseranwendungen – Untersuchung der optischen Gewebeeigenschaften und physikalisch-mathematische Modellbildung* (Ecomed, Landsberg 1997)
26. P. Kubelka, F. Munk: Z. Tech. Phys. **12**, 593 (1931)
27. K.M. Case, P.F. Zweifel: *Linear Transport Theory* (Addison-Wessley, London 1967)
28. T.J. Farell, M.S. Patterson, B.C. Wilson: Med. Phys. **19**(4), 879 (1992)
29. G. Yoon, S. Prahl, A.J. Welch: Appl. Opt. **28**(12), 2250 (1989)
30. N. Metropolis, N. Ulam: J. Am. Stat. Asc. **44**, 335 (1949)

31. B.C. Wilson, G. Adam: Med. Phys. **10**(6), 824 (1983)
32. G.J. Mueller, A. Roggan (Eds.): *Laser-induced Interstitial Thermotherapy* (SPIE Press, Bellingham 1995)
33. C.T. Germer, A. Roggan, J.P. Ritz, C. Isbert, D. Albrecht, G. Mueller, H.J. Buhr: Lasers Surg. Med. **23**(4), 194 (1998)
34. R. Splinter, W.F. Cheong, M.J.C. van Gemert, A.J. Welch: Lasers Surg. Med. **9**, 37 (1989)
35. D.J. Maitland, J.T. Walsh, J.B. Prystowsky: Appl. Opt. **32**(4), 586 (1993)
36. R. Marchesini, E. Pignoli, S. Tomatis, S. Fumagalli, A.E. Sichirollo, S. Di Palma, M. Dal Fante, P. Spinelli, A.C. Croce, G. Bottiroli: Lasers Surg. Med. **15**, 351 (1994)
37. I.F. Cilesiz, A.J. Welch: Lasers Surg. Med. **14**, 396 (1994)
38. Hereaus product information on Suprasil glass (1995)
39. F.P. Bolin, L.E. Preuss, R.C. Tylor, R.J. Ference: Appl. Opt. **28**(12), 2297 (1989)
40. E. Gordy, D.L. Drabkin: J. Biol. Chem. **227**, 285 (1957)
41. B.C. Wilson, M.S. Patterson: Phys. Med. Biol. **31**, 327 (1986)
42. M.R. Arnfield, R.P. Mathew, J. Tulip, M.S. McPhee: Phys. Med. Biol. **37**, 1219 (1992)
43. J.F. Beek, P. Blokland, P. Posthumus, M. Aalders, J.W. Pickering, H.J. Sterenborg, M.J.C. van Gemert: Phys. Med. Biol. **42** (11), 2255 (1997)
44. I.F. Cilesiz, A.J. Welch: Lasers Surg. Med. **14**, 396 (1994)
45. A. Roggan, M. Friebel, K. Dörschel, A. Hahn, G. Müller: J. Biomed. Opt. **4**(1), 36 (1999)